Righting and turning in mid-air using appendage inertia: reptile tails, analytical models and bio-inspired robots

2010 Bioinspir. Biomim. 5 045001

(http://iopscience.iop.org/1748-3190/5/4/045001)

Bioinsp. Biomim. **5** (2010) 045001 (12pp) doi:10.1088/1748-3182/5/4/045001

Righting and turning in mid-air using appendage inertia: reptile tails, analytical models and bio-inspired robots

A Jusufi[1], D T Kawano[2], T Libby[3] and R J Full[1]

[1] Department of Integrative Biology, University of California, Berkeley, CA 94720-3140, USA
[2] Department of Mechanical Engineering, University of California, Berkeley, CA 94720-1740, USA
[3] Center for Interdisciplinary Bio-inspiration in Education and Research, University of California, Berkeley, CA 94720-3140, USA

E-mail: ardianj@berkeley.edu

Received 7 June 2010
Accepted for publication 24 August 2010
Published 24 November 2010
Online at stacks.iop.org/BB/5/045001

Abstract
Unlike the falling cat, lizards can right themselves in mid-air by a swing of their large tails in one direction causing the body to rotate in the other. Here, we developed a new three-dimensional analytical model to investigate the effectiveness of tails as inertial appendages that change body orientation. We anchored our model using the morphological parameters of the flat-tailed house gecko *Hemidactylus platyurus*. The degree of roll in air righting and the amount of yaw in mid-air turning directly measured in house geckos matched the model's results. Our model predicted an increase in body roll and turning as tails increase in length relative to the body. Tails that swung from a near orthogonal plane relative to the body (i.e. 0–30° from vertical) were the most effective at generating body roll, whereas tails operating at steeper angles (i.e. 45–60°) produced only half the rotation. To further test our analytical model's predictions, we built a bio-inspired robot prototype. The robot reinforced how effective attitude control can be attained with simple movements of an inertial appendage.

S Online supplementary data available from stacks.iop.org/BB/5/045001/mmedia

(Some figures in this article are in colour only in the electronic version)

1. Introduction

Animals in arboreal habitats can lose footholds and fall as a consequence of challenging terrain, predator–prey interactions, fighting behavior or mating [1–4]. While in free fall many can reorient themselves to a posture in which their ventral side faces the ground, thereby decreasing the possibility of injury, permitting effective maneuvering and/or avoiding undesirable environments. The notion that animals can perform righting in mid-air without pushing themselves off the substrate beforehand or without changes in net angular momentum was contested in the 19th century. The dispute was first experimentally addressed in 1894 by a study of the falling cat [5]. The cat's air-righting responses are generally characterized by twisting and bending between the anterior and the posterior parts of the torso [5–11], changing shape and instantaneous moment of inertia [12]. The study of air-righting reactions has mainly focused on mammals, such as cats, monkeys, guinea pigs, rabbits and rats [5–14]. Animals can use mass redistribution by their appendages to induce zero-angular momentum reorientations in mid-air [e.g. 8–11, 15]. The extent to which the limbs contribute to self-righting in falling cats is still under-explored [10]. Because it was observed that the tail rotates when the cat rights itself, it was proposed that the tail could be used for at least the fine-tuning of the air-righting reaction. However, in a comparison between the air-righting performance of tailed and tailless cats, no difference could be found [7]. Mammals with relatively small tails, such as rabbits and guinea pigs, appear to right themselves predominately by twisting [13, 14]. Mammals

with longer tails, such as rats, can still perform aerial righting if either head-torso or torso-pelvis remains free for rotation. However, if head-torso and torso-pelvis rotation is prevented, leaving only the tail free to move, the rats are incapable of attaining a right-side-up posture [13]. Righting with the tail alone has not yet been found in mammals. Primates have been hypothesized to use rotation of their tails to assist in leaping maneuvers [16, 17] and more generally to maintain balance during arboreal locomotion on narrow branches [18]. Whether 'flying squirrels' use their tail as a steering device during gliding is unknown [19].

Because reptiles tend to have larger and more massive caudal appendages than mammals, their tails could be used to change body orientation. Tail motion in lizards has been observed during simulated [20] and actual free fall [21]. Tail cycling during free fall of the 'flying gecko' has been associated with changes in posture such as somersaulting [22]. Movement of the tail has been reported to affect the turning ability of tailed [23] and tailless [24] jumping green anoles, *Anolis carolinensis*. From free fall in an upside-down posture, flat-tailed house geckos *Hemidactylus platyurus* swing their tail nearly perpendicular to their body, 180° in one direction to cause their body to rotate 180° in the other (figure 1; see movie 1 available at stacks.iop.org/BB/5/045001/mmedia) [25]. By conserving angular momentum, house geckos can right themselves rapidly in mid-air, attaining a right-side up, gliding posture [25]. While descending in the gliding posture, house geckos can yaw to produce a turn by further swings of their tail.

Here, we develop an analytical model to investigate the effectiveness of tails as inertial appendages that can change body orientation. We anchored our model by measuring the relevant morphological parameters for the well-studied, flat-tailed house gecko *H. platyurus*. This approach allowed direct testing of the model with previously measured kinematic results from mid-air righting and turning [25]. Using the house gecko as a starting point, we then explored the parameter space reflecting the variation we see in this species. We examined the model's air-righting and turning performance as we varied two parameters—the tail length and the inclination angle relative to the body. By extending beyond this space, we speculate about the effectiveness of designs that begin to represent other species that can use their tails for reorientation. Finally, we applied the model predictions to a robot prototype of one of the most successful legged, climbing robots [26] yet built to test if it could right in mid-air using only its tail.

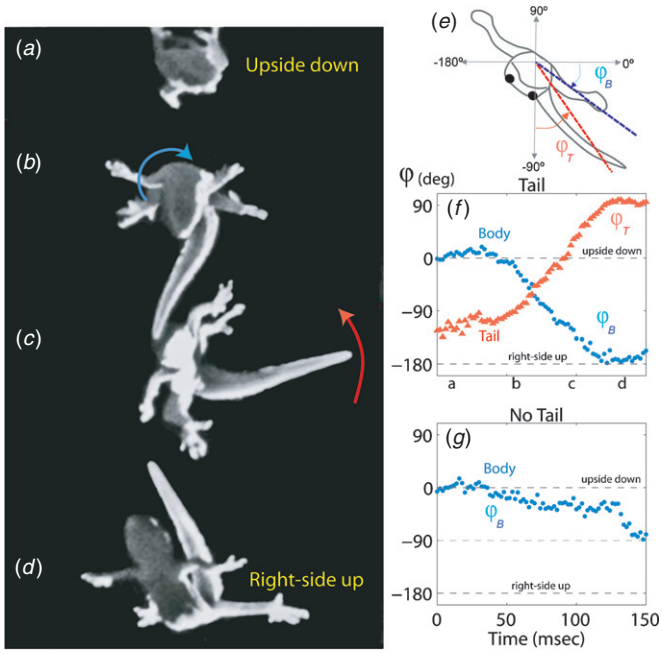

Figure 1. Air-righting maneuver in a gecko with intact and autotomized tails. Flat-tailed house gecko *H. platyurus* in free fall. (*a*) Geckos took off from platform in supine posture. (*b*) Animals free fall in upside-down posture for approximately 45 ms. (*c*) The onset of tail and body rotation occurs simultaneously. (*d*) Tail ceases to rotate when body reaches near horizontal posture sufficient for landing. The tail (red arrow) rotates clockwise and the body (blue) anti-clockwise. (*e*) Axes of rotation defined. (*f*) Rotation of body (•, φ_B) and tail (▲, φ_T) rotation during air-righting maneuver as a function of time. (*g*) Body rotation (•, φ_B) in tailless animals during an attempted air-righting maneuver as a function of time. Modified from [25], copyright (2008) National Academy of Sciences, USA.

2. Materials and methods

2.1. Model design and parameters

To investigate the feasibility of righting the body from upside-down to right-side-up posture by way of circular tail motion in the plane orthogonal to the axis of body roll, we developed a simple theoretical model anchored in the morphology of the house gecko, *H. platyurus*.

Multi-segment models that conserve angular momentum while righting in mid-air have been discussed in the literature to describe the motion of falling cats [8, 10, 11, 28], robots of various designs [27, 29], humans in space [15, 30] and even cell phones [31]. The models presented in these papers range from two jointed rigid bodies [28, 29, 31] to elaborate multi-segment and multi-jointed bodies [10, 30], with some focusing on the design of a specific physical robot [27] or specializing in the morphology of cats [10] or humans [30]. Several of these studies [10, 28, 29, 31] are control oriented, often concerned with determining an optimal control sequence to produce a desired air-righting response. Consequently, the derivations of the associated equations of motion (differential-algebraic equations [10], a Lagrangian approach [31], etc), geared toward an optimal control problem, often lack the simplicity we desire to simply verify experimental observations of gecko righting and then use experimental findings to predict righting behavior. We chose a jointed two-body model of the gecko righting (similar to the models in [28] and [31]) for its ease of formulation, and where the equations of motion are most efficiently obtained through basic vector mechanics by conserving angular momentum about the system's mass center (see equation (2) in [30], replacing 10 with 2 for the number of jointed bodies). Our model is, in essence, a simplified two-body version of the ten-body human model in [30], with one of the bodies tailored to the morphology of the house gecko's body (torso and legs) and the other body representing the tail.

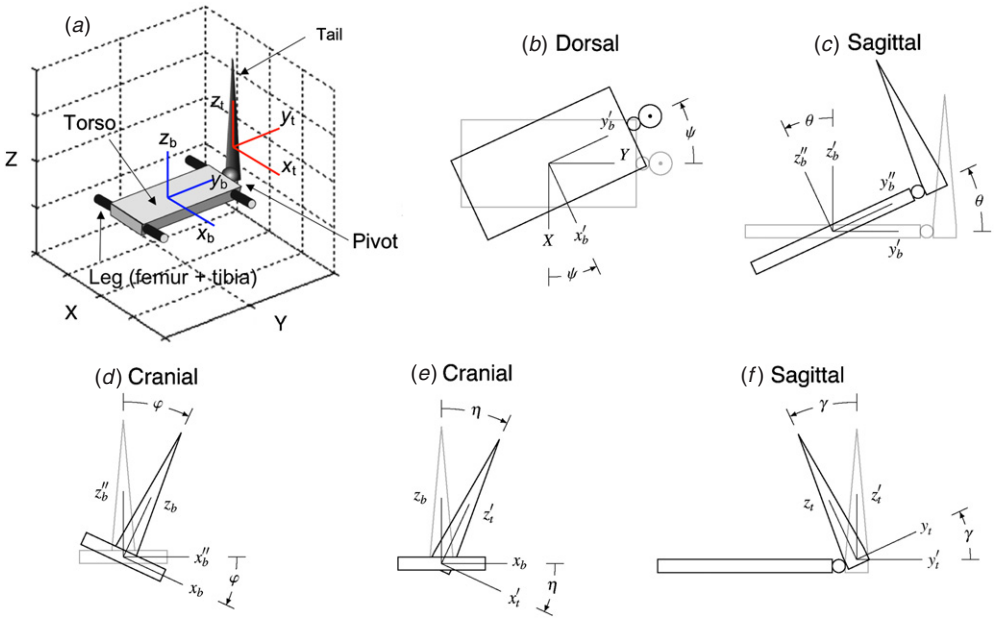

Figure 2. Analytical model planar views illustrating the sequence of rotations for the gecko model's body and tail from the fixed XYZ frame to the body-fixed $x_b y_b z_b$ frame and tail-fixed frame $x_t y_t z_t$. (*a*) 3D view of the analytical model of the house gecko. (*b*) Dorsal view of the body yaw ψ. (*c*) Sagittal view of the body pitch θ. (*d*) Cranial view of the body roll φ. (*e*) Cranial view of the tail side sweep η relative to the body. (*f*) Sagittal view of the tail inclination γ relative to the body.

We represented the gecko as two rigid bodies, one for the torso and legs, and the other for the tail (figure 2(*a*)). Based on experimental observations of geckos righting in mid-air, we believe that treating the body as a single rigid component is a reasonable approximation, since significant flexing of the gecko's torso does not occur, unlike the traditional problem of the falling cat. The body (torso and legs) and tail were connected by a small universal joint that prohibited lengthwise spin of the tail. We assumed that momentum was completely transferred from the tail to the body across the joint. We modeled the tail as a cone. The torso was modeled as an elliptical slab with widths (the major axis) and heights (the minor axis) measured directly from the animals. The value for the major axis takes into account variations in torso width from snout to tail base. We used cadavers to determine the effective radii at the snout, forehead, neck, shoulder, breast, rib cage, pelvis and tail base. To explore the inertial properties of the limbs, we modeled the front and rear legs as cylinders and we assumed that the femoral segments were protracted maximally away from the longitudinal body axis. We chose the body-fixed axes $x_b y_b z_b$ and tail-fixed axes $x_t y_t z_t$ so that the body and tail were symmetric relative to their respective axes (i.e. there are no products of inertia for the body and tail (see figure 2(*a*))).

To obtain the theoretical model, we derived an expression for the total angular momentum $\mathbf{H}$ about the gecko's mass center using vector mechanics (equation (2) in [30], replacing 10 with 2 for the number of bodies). We calculated the angular momenta about the mass centers of the body and tail by considering a rotation sequence of the yaw ψ, then the pitch θ, then the roll φ of the body and tail (i.e. a 3–1–2 set of Euler angles), followed by the side sweep η and the inclination γ of the tail relative to the body (see figures 2(*b*)–(*f*) for an illustration of the rotation sequence).

We assumed that when a gecko performs self-righting during free fall, no external torques are acting on the system and therefore angular momentum is conserved: $\mathbf{H}$ = constant = $\mathbf{0}$ when the gecko is released from rest. Aerodynamic effects were assumed to be negligible in the model due to the following considerations. To investigate the possibility of aerodynamic forces affecting the air-righting maneuver, we performed calculations that were based on conservative overestimates, such as the cross-sectional area subjected to airflow and the drag coefficient (see appendix A for details). The calculations suggest that the maximum drag moment from aerodynamic forces acting on the tail could account for only 3.6% of the total moment that the geckos require to perform air righting successfully. The low percentage for the drag moment relative to the inertial moment indicates that non-inertial torques are less likely to play a major role in this behavior.

Writing the three components of the angular momentum vector with respect to the body-fixed frame $x_b y_b z_b$ in matrix-vector form, the gecko model's aerial rotation is governed by

$$\mathbf{A}\dot{\mathbf{y}} = \mathbf{f}_1\dot{\eta} + \mathbf{f}_2\dot{\gamma},$$

$$\begin{bmatrix} A_{11} & A_{12} & A_{13} \\ A_{21} & A_{22} & A_{23} \\ A_{31} & A_{32} & A_{33} \end{bmatrix} \begin{bmatrix} \dot{\psi} \\ \dot{\theta} \\ \dot{\varphi} \end{bmatrix} = \begin{bmatrix} f_{11} \\ f_{12} \\ f_{13} \end{bmatrix} \dot{\eta} + \begin{bmatrix} f_{21} \\ f_{22} \\ f_{23} \end{bmatrix} \dot{\gamma}, \qquad (1)$$

for which the superposed dot denotes a time derivative. The components A_{ik} (i, k = 1, 2, 3) of the coefficient matrix $\mathbf{A}$, f_{1i} (i = 1, 2, 3) of the vector $\mathbf{f}_1$ associated with the tail side sweep and f_{2i} (i = 1, 2, 3) of the vector $\mathbf{f}_2$ associated with tail inclination for equation (1) are derived in appendix B. We show the model's inputs and outputs in table 1. We performed

Table 1. Input and output parameters of the analytical model for testing tail-induced body reorientation.

Property	Description
Input parameters:	
J_{bi} $(i = 1, 2, 3)$	Body moments of inertia
J_{ti} $(i = 1, 2, 3)$	Tail moments of inertia
m	Ratio of body mass × tail mass to total mass
L_1	Body mass center to tail base center distance
L_2	Tail base center to tail mass center distance
$\eta(t)$	Tail side sweep profile
$\gamma(t)$	Tail incline profile
$\psi_0, \theta_0, \varphi_0$	Initial body orientation
Output parameters:	
$\psi(t)$	Body yaw over time
$\theta(t)$	Body pitch over time
$\varphi(t)$	Body roll over time

Table 2. Masses, dimensions and inertial properties of geckos' torso, tail and legs.

Property	Mean	Standard deviation
Torso mass (kg)	2.9×10^{-3}	$\pm 5.1 \times 10^{-4}$
Tail mass	2.9×10^{-4}	$\pm 8.9 \times 10^{-5}$
Fore leg mass	9.8×10^{-5}	$\pm 7.3 \times 10^{-6}$
Rear leg mass	1.9×10^{-4}	$\pm 1.2 \times 10^{-5}$
Body length (m)	5.4×10^{-2}	$\pm 6.4 \times 10^{-3}$
Body semi-major axis	4.2×10^{-3}	$\pm 3.8 \times 10^{-4}$
Body semi-minor axis	3.7×10^{-3}	$\pm 3.6 \times 10^{-4}$
Tail length	5.0×10^{-2}	$\pm 8.2 \times 10^{-3}$
Tail base radius	4.0×10^{-3}	$\pm 4.0 \times 10^{-4}$
Fore leg femur length	7.6×10^{-3}	$\pm 6.8 \times 10^{-4}$
Fore leg femur width	3.1×10^{-3}	$\pm 2.0 \times 10^{-4}$
Fore leg shank length	7.5×10^{-3}	$\pm 1.8 \times 10^{-4}$
Fore leg shank width	2.8×10^{-3}	$\pm 3.6 \times 10^{-4}$
Rear leg femur length	9.0×10^{-3}	$\pm 6.6 \times 10^{-4}$
Rear leg femur width	5.9×10^{-3}	$\pm 5.1 \times 10^{-4}$
Rear leg shank length	8.6×10^{-3}	$\pm 3.9 \times 10^{-4}$
Rear leg shank width	2.8×10^{-3}	$\pm 8.5 \times 10^{-5}$
Body pitch moment of inertia (MOI), J_{b1} (kg m^2)	1.1×10^{-6}	$\pm 4.4 \times 10^{-7}$
Body roll MOI, J_{b2}	6.6×10^{-8}	$\pm 1.0 \times 10^{-8}$
Body yaw MOI, J_{b3}	1.2×10^{-6}	$\pm 4.4 \times 10^{-8}$
Tail pitch MOI, J_{t1}	3.0×10^{-8}	$\pm 1.8 \times 10^{-8}$
Tail roll MOI, J_{t2}	3.0×10^{-8}	$\pm 1.8 \times 10^{-8}$
Tail yaw MOI, J_{t3}	1.4×10^{-9}	$\pm 6.4 \times 10^{-10}$

all calculations with standard software (Mathematica and MATLAB). We determined the moments of inertia using dimensions taken from cadavers (table 2). We measured the torso and tail mass, snout–vent length, tail length and radius from six *H. platyurus* individuals. We measured leg lengths from four individuals. We performed statistics using standard software (JMP and Microsoft Excel).

To calculate the moment of inertia of the torso, we modeled the body as an elliptical slab with major axis and minor axis. The dorso-ventral body height (minor axis) was approximately uniform across the torso. To determine the lateral width (major axis), we used an average value from the snout to tail base. In *H. platyurus* the maximum lateral radius (major axis) was measured at the rib cage whereas the minimum values were found at the snout and the tail base. We dissected cadavers of *H. platyurus* to investigate the inertial properties of the geckos' legs and measured the masses and dimensions of the femora and tibiae of each fore and rear leg ($n = 4$).

From the average and standard deviation of the estimated moments of inertia for the body and tail calculated from biometric data (see table 2), we observed that there was significant variation in the moments of inertia associated with roll of the gecko body (J_{b2}) and turning of the tail (J_{t1} and J_{t2}). Of the system's six moments of inertia, these three have the greatest effect on the gecko's aerial righting performance because they primarily govern the reorientation (i.e. roll). By using average values for the moments of inertia, we would obtain results that are not representative of the actual performance of the individual specimens. For this reason, in our investigation of the effect of the relative tail length and tail inclination we chose to focus on model results for a single specimen whose body morphology (i.e. ratio of tail length to snout–vent length) was nearest to the average values across all individuals (1.08 ± 0.18, $n = 6$).

To ground our speculation of how other species with varying body and tail lengths may perform mid-air righting and turning, we collected morphological data on anoles. The average body length of the *A. carolinensis* was 5.3×10^{-2} m $\pm 1.3 \times 10^{-3}$ m ($n = 3$, snout–vent length). We measured tail lengths that well exceed the snout–vent length of the animals: 9.53×10^{-2} m with a standard deviation of 6.7×10^{-3} m ($n = 3$). The average body mass of the anoles was 3.0×10^{-3} kg $\pm 1.1 \times 10^{-3}$ kg.

2.2. Air righting

The initial conditions for the aerial righting simulation correspond to the house gecko starting upside down with no pitch and yaw: $\psi_0 = \theta_0 = 0^\circ$, $\varphi_0 = -180^\circ$. To ensure that the gecko has no initial angular momentum, the profiles for the tail side sweep $\eta(t)$ and tail incline $\gamma(t)$ must be chosen so that they yield zero initial angular velocity (i.e. $\dot{\eta}(0) = \dot{\gamma}(0) = 0$). Since angular momentum is conserved, it follows that the final values of angular velocity must also be zero so that the gecko stops rotating. We examined the aerial righting motion of the house gecko (*H. platyurus*) by first making a direct comparison with the air-righting data and then by varying two parameters—tail length relative to body length and the tail inclination angle.

2.2.1. Varying tail length relative to body length. We studied the effect of tail length on the righting behavior of a house gecko (*H. platyurus*) of representative dimensions with a nominal tail length of 5.4 cm and a body length of 4.59 cm. The tail length was varied from the shortest measured gecko tail length of 4 cm to the longest measured value of 6.1 cm. We extended the simulation results by including tail to body length ratios that fall within the range of *A. carolinensis*. We varied tail lengths for a tail rotating one revolution relative to the body when the tail was held orthogonal to the body. In the case where there was no tail inclination ($\gamma = 0^\circ$), we

prescribed the relative sweep of the tail by a half-cosine with a duration of 110 ms (an average value based on experimental observations) to approximate the experimentally determined tail sweep trajectory in figure 1(f).

2.2.2. Varying tail inclination γ. We next explored how the body roll, as a function of tail length, would be affected if the tail was not held orthogonal to the body plane, but rather at a fixed incline so that the tail swept out a cone relative to the body. We examined the roll performance for various tail to body length ratios using tail inclination angles of 15°, 30°, 45° and 60°.

2.3. Turning

To examine turning of the gecko's body due to tail sweep in the horizontal XY plane, we set the first tail angle η to a constant $-90°$ so that the tail was constrained to rotate in the XY plane according to $\gamma(t)$ which then described planar yaw of the tail instead of inclination as before. We used a half-cosine profile for $\gamma(t)$ to ensure conservation of (zero) angular momentum (figure 1(f)). The initial conditions were chosen so that the body had no initial yaw in the XY plane (i.e. $\psi_0 = \theta_0 = \varphi_0 = 0°$).

2.3.1. Varying tail length relative to body length. We studied how the planar yaw of the gecko was affected by both the tail to body length ratio and the amount of relative sweep of the tail. We varied the tail length from 4 cm to 6.1 cm (i.e. the range of measured values for the house gecko specimens), and the relative motion of the tail ranged from 30° to 180° in increments of 30°. In all cases, the tail was initially held orthogonal to the length of the body.

2.4. Model scaling

To compare body reorientation across different tail lengths, we scaled the tail length and the tail base radius isometrically to keep density constant (see section 3.3, as mass scales cubically with the tail length ratio α). A cylinder tapering toward one tip was a reasonable shape to approximate the moment of inertia of the tail, assuming constant density across the various tissues that make up the caudal appendage. We also reasoned through the effects of isometric scaling on air-righting and turning performance to make predictions about lizards as well as our larger robot prototype.

2.5. Robot prototype

To test the hypothesis that righting could be accomplished with a purely zero angular momentum approach, we built a simple, scaled-up robot prototype (figure 5(d)). The robot consisted of a solid body constructed from laser-cut acrylic and aluminum sheet connected to an acrylic tail via a single revolute joint. We actuated the tail by using a torsion spring-loaded shaft which was preloaded and locked with a pin. The robot was a scaled and proportioned version of a bio-inspired quadrupedal robot [26] designed to climb. We used a tail stroke relative to the body of approximately 360°, as was observed in the house geckos (*H. platyurus*). The tail moment of inertia was made sufficiently large by placing a 14 g lead weight 22 cm from the body axis.

Table 3. Mass, dimensions and inertial properties of robot prototype.

Property	Body	Tail
Mass (kg)	2.14×10^{-1}	4.80×10^{-2}
Center of mass distance from joint (m)	1.65×10^{-1}	1.95×10^{-1}
Pitch moment of inertia (MOI) (kg m^2)	2.4×10^{-3}	6.0×10^{-4}
Roll (MOI)	6.5×10^{-4}	6.0×10^{-4}
Yaw (MOI)	2.9×10^{-3}	5.0×10^{-6}

During initial testing, the final position of the mass was modulated to fine-tune body rotation. The robot was dropped and video recorded with a high-speed video camera (AOS X-PRI, AOS Technologies AG). If under- or over-rotation of the body was observed, we modulated the moment of inertia of the tail by changing the moment arm of the mass on the tail. Time course of rotation was controlled via the strength of the torsion spring. To end the maneuver, we employed a damped bump-stop (i.e. a sticky tack on steel) to halt the rotation without a rebound. A viscoelastic foam pad prevented damage to the robot on landing.

A delayed release pin controlled initiation of righting as follows. We preloaded the tail, hung the robot upside down and secured it with a release pin. We locked the preloaded tail using a pin tied to a length of string. Both release mechanisms consisted of a steel pin in a Teflon bearing to keep friction at a minimum as the pin slides out. When the body pin was removed, the robot fell, and at a distance of 10 cm, the string pulled the tail release pin, initiating tail rotation. This approach ensured that no external torques would be introduced during the release. If the tail accelerated while the body was contacting the substrate, net angular momentum would be introduced and the righting would not be stable. For the same reason, the release pin bearing was positioned at the center of mass of the model such that friction forces could not impart a moment to the body.

We used the same analytical model described previously (see section 2.1) to make predictions about the robot's performance. Because the robot's mass distribution varied significantly from the animals, we directly measured its physical parameters rather than estimating them from segment lengths. We measured the mass, centers of mass and mass moments of inertia about the three principle axes of both the body and tail of the physical model (see table 3). We measured moments of inertia with a bifilar pendulum constructed by suspending the robot by lengths of string. We fixed the tail inclination angle at 35° from vertical. We chose the tail side-sweep kinematics to be a half-cosine as in the animal model. However, we used a duration of 250 ms (based on experimental observations) and the actual measured tail stroke of 309° relative to the body's rotation instead of a complete rotation.

3. Results and discussion

Lizards, such as geckos, can use their tails to perform maneuvers at the interface of terrestrial and aerial locomotion with exceptional precision and agility [23–25]. Contrary to the falling cat [5–11] and other quadrupedal mammals [12, 13], no head–shoulder or shoulder–pelvis twist appears to be required for sufficient air righting in flat-tailed house geckos *H. platyurus*. We define sufficient righting to be body roll that falls within the range of 140–180° as was observed in all experimental trials in geckos ($n = 16$; [25]). Preliminary results in anoles indicate that they also fall in this range. Examining the experimentally measured angular position of the pelvis and shoulder over time in the house gecko reveals that the body does not twist (figure 1) in most trials. By making the fore and hind portions of the body rigid and coplanar in an analytical model and a robot prototype, we show that sufficient mid-air righting is possible.

Not only does our analytical model and robot prototype show that tail movement alone is sufficient for aerial maneuvers, but they also raise the hypothesis that external forces, such as aerodynamic lift and drag, are not required. Because air righting occurs within a vertical height of less than two body lengths, well before the animal achieves terminal velocity, lift- and drag-based mechanisms for righting appear less likely. However, as both the tail and body can achieve high angular velocities during the maneuver, significant drag may act on both segments. Yet, the kinematics of air righting in both animals and the robot showed little or no change in angular momentum during maneuvers, suggesting that the net impulse due to drag is negligible. In addition, conservative overestimates of the maximum moment that could be induced by drag forces acting on the tail indicate that aerodynamic effects are small (see section 2.1). The drag moment could account for only 3.6% of the total maximal moment necessary to reorient the body (see appendix A), thus suggesting that inertia is the main component. Although challenging, a next step in model development should include drag forces.

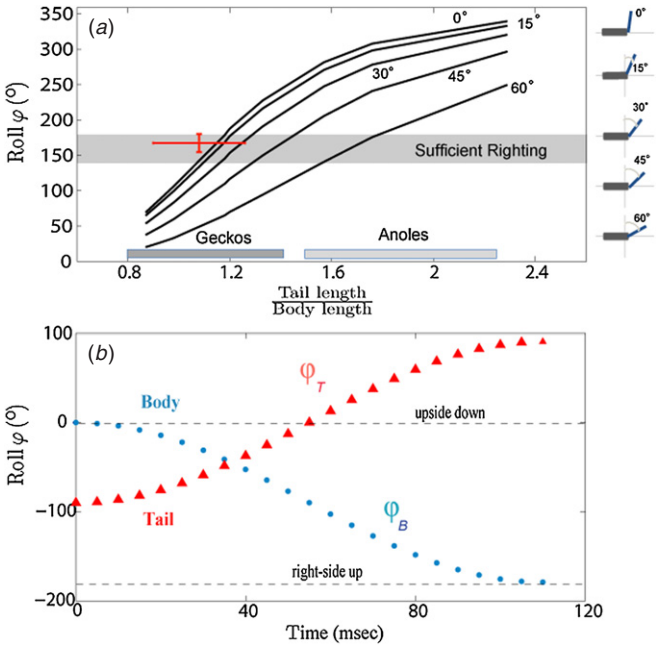

Figure 3. Effect of tail length and inclination on induced body roll. (*a*) Tail-induced body roll as a function of the tail length to body length ratio for the tail held at an angle of 0°, 15°, 30°, 45° and 60° relative to the vertical, as depicted by the icons from top to bottom. The shaded region denotes the range of near-prone posture for sufficient air righting to right-side-up posture. The red cross represents measurements from the air-righting experiments with house geckos (*H. platyurus*). The vertical red line indicates the final position of the body relative to the horizontal during air righting (mean ± 1 s.d.). The horizontal red line indicates the tail length to body length ratios observed in house geckos (mean ± 1 s.d.). The grey bars show the range of tail to body lengths found in house geckos and green anoles. The plot shows the variation in body roll for a gecko of average dimensions when the tail makes one full revolution relative to the body. All other body parameters were held fixed. Tail lengths used for calculation span the range of measured house gecko tail lengths to hypothetical lengths that approach those in lizards such as anoles. We scaled the tail length and the tail base radius isometrically to keep density constant. (*b*) Depicted is the righting performance of the average house gecko as predicted by the analytical model. The rotations of the body (•, φ_B) and the tail (▲, φ_T) are plotted as a function of time (see figure 1(*f*)).

3.1. Air-righting model

Our analytical model of a representative flat-tailed, house gecko predicted the air-righting performance measured in the animals. Rotation of the tail in one direction elicited righting behavior (roll) in the body in the opposite direction. As observed in the animals, rotations about other axes (pitch and yaw) were small in comparison to the roll achieved, and angular momentum was zero both before and after the maneuver. To make comparisons between individuals and the model, we normalized absolute tail rotation by absolute body rotation. The ratio of absolute tail rotation to absolute body rotation ($\Delta\varphi_T/\Delta\varphi_B$) expresses the tail effort required for righting—animals that use more tail rotation to achieve righting will have a higher ratio. If conservation of angular momentum is the primary mechanism for righting in lizards, the model should predict the ratio of rotation observed in the experimental trials. We used a *t*-test of paired means to determine the match of the experimental results to the model prediction. The difference between the two ratios was not statistically significant ($P > 0.2$, *t*-test of paired means, $n = 6$, and is further supported by $P > 0.2$ with a Wilcoxon test). This suggests that the gecko's tail is capable of generating sufficient moment to account for a reorientation of its body. The model predicted a ratio of 1.24 ± 0.22 (mean ± s.e., $n = 6$), whereas the experiments on geckos produced a value of 1.26 ± 0.20 ($n = 6$).

3.1.1. Varying tail length relative to body length. Because the house gecko *H. platyurus*, and lizards in general, vary in the length of their tail relative to the length of their body, we used our analytical model to predict the degree of reorientation or roll as the tail length to body length ratio varied (figure 3(*a*)). The model predicts that the degree of body roll during air righting will increase as the tail length relative to body length increases.

First, we used the model to examine the effect of the natural variation in the house gecko tail to body length ratio (i.e. 0.8–1.33) on air-righting performance. If average house geckos *H. platyurus* (tail length 5.4 cm, tail length/body length = 1.18) can sweep their tail 360° relative to the body, then the model predicts that they should be able to right themselves sufficiently from an upside-down to a near-right side-up pose for landing (see movie 2 available at stacks.iop.org/BB/5/045001/mmedia), as long as they keep their tail inclination angle less than 45° (figure 3(*b*); see cross). The tails of house geckos that are 20% longer (tail length = 6.1 cm, tail length/body length = 1.33) and swung at a zero degree inclination angle (i.e. orthogonal to the body plane) are predicted to generate 50° more body roll (i.e. 229°) with one tail swing.

Second, we explored the parameter space beyond the house gecko to predict how further increases in the tail length might affect righting performance (figure 3(*a*)). If the lizard tail were nearly twice as long as the body (tail length = 10.5 cm, tail length/body length = 2.29) and made one revolution with respect to the body, then the body roll would nearly double to 341°. Preliminary observations suggest that much smaller rotations of the tail (less than 45° absolute rotation) are sufficient to effect righting in lizards with tail lengths substantially greater than body lengths, such as in green anoles (average tail length = 9.35 cm, tail length/body length = 1.8). Thus, our model predicts and preliminary experiments suggest that a longer tail will be a considerably more effective inertial appendage for reorientation, as lizards require less effort to achieve aerial righting of their body.

3.1.2. Varying tail incline γ. We noted that house geckos *H. platyurus* did not always hold their tail in a plane orthogonal to the body when swinging it to perform air righting. When the tail is not held orthogonal to the body (i.e. more than 0°), it sweeps out a more conical trajectory. Our analytical model showed that a lizard's ability to generate roll during air righting decreased if its rotating tail was not held perpendicular to the body (figure 3(*a*)). The model predicts that if the tail of the average gecko is not held orthogonal to the axis of rotation, but is inclined by 15°, then the body will still reorient sufficiently to a 170° roll angle. If the tail is inclined by 30°, then the model predicts that the body will reorient to a 146° roll angle, which will be just sufficient to allow for a successful landing or transition to gliding. However, the model predicts that if the tail of the average house gecko is inclined by 45° or more, then air righting will be unsuccessful as the body will reorient to only 110° or less. Righting is unsuccessful even with this longest gecko tail (tail length/body length = 1.33) if it is inclined by 60°, since the model predicts that the body will reorient only halfway to 95°, as can be seen in simulation (movie 3 available at stacks.iop.org/BB/5/045001/mmedia). The house gecko with the shortest tail (tail length = 4 cm, tail length/body length = 0.8) will roll only 70° if the tail only makes one revolution with respect to the body. By contrast, a lizard tail that is twice as long (tail length = 8.1 cm, median length for green anoles, tail length/body length ratio of 1.76) permits the animal to hold it at an inclination of 60° and still fully reorient its body to 176°, as can be seen in simulation (movie 4 available at stacks.iop.org/BB/5/045001/mmedia).

In preliminary mid-air righting experiments using the green anole, *A. carolinensis*, we observed the tail being held at a particularly exaggerated angle (i.e. more than 45° from vertical). Our model predicts that if a lizard with a long tail (tail length/body length = 1.57), such as the green anole, makes one revolution with respect to the body, it can incline the tail at a steep angle of 60° and still reorient its body to 141° of roll, thus attaining a sufficient near-prone posture (figure 3(*a*), see movie 5 available at stacks.iop.org/BB/5/045001/mmedia). Our observations of righting in anoles indicate that they achieve complete righting despite their relatively large tail inclination.

Green anoles may be restricted in the extent to which they can position and swing their tail. The hind legs of *A. carolinensis* are nearly twice as long as the fore legs. The ratio of hind leg to fore leg length is much larger than in the house gecko *H. platyurus*. Further study is needed to test the hypothesis that lizards, such as anoles, might be constrained in their tail movements to avoid collisions with their hind legs.

3.2. Turning

Upon completion of air righting, we observed that flat-tailed, house geckos used movements of the tail during aerial descent [25]. To test whether tail activity played a role, we simulated equilibrium gliding conditions by using a vertical wind tunnel (see [25] for more details about the wind tunnel experiments). *H. platyurus* attained terminal velocity at ventral airflows ranging from 4.0 m s^{-1} to 7.0 m s^{-1}. We observed that tail movements occurred simultaneously with systematic turning maneuvers. In addition to large 90° turns that correlated with circular tail motion, we found that geckos could also generate smaller turns of the body in the yaw plane (see movie 6 available at stacks.iop.org/BB/5/045001/mmedia). For these smaller turns, geckos kept both the body and tail in the horizontal plane (i.e. *XY* plane), thus conserving momentum about an axis perpendicular to that plane. A similar use of the tail for turning has been proposed for *Anolis* lizards in the airborne phase of jumping [23]. Therefore, to investigate the effectiveness of tails to induce mid-air turning, we viewed our analytical model in an *XY* plane projection and set the initial conditions for zero yaw.

3.2.1. Effect of tail length relative to body length. First, we used our analytical model to predict the degree of mid-air turning (yaw) as we varied the length of the tail relative to the length of the body within the natural variation measured in the house gecko *H. platyurus* (figure 4). The model predicts that the degree of body yaw will increase as the tail length relative to the body length increases. For the average gecko (tail length 5.4 cm, tail length/body length = 1.18) the model predicts that if the tail sweeps 180° in one direction relative to the body, the gecko will complete a turn of about 20° in the other direction (figure 4), which is consistent with the observed results. Geckos with the largest relative tail lengths could generate nearly twice as much body yaw than geckos with the shortest tails.

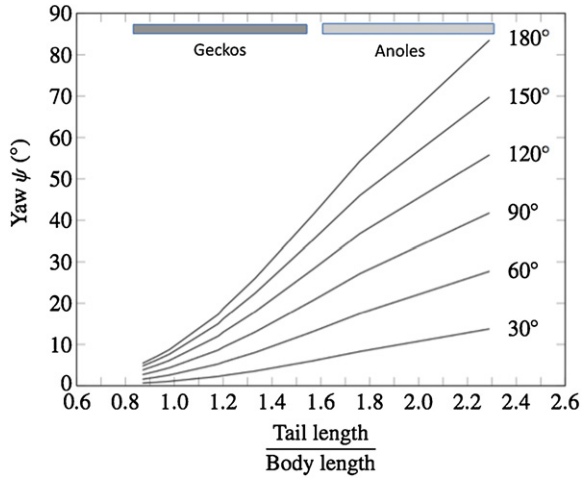

Figure 4. Mid-air turning performance as a function of tail length relative to body length and the degree of tail sweep. The plot shows the variation in body yaw for a gecko of average dimensions when the tail is swung in the plane of the body. The tail sweeps from 30° to 180° in 30° intervals. Tail lengths used for calculation span the range of measured house gecko tail lengths to hypothetical lengths that approach those in lizards such as anoles, as indicated by the grey bars. All other body parameters were held fixed.

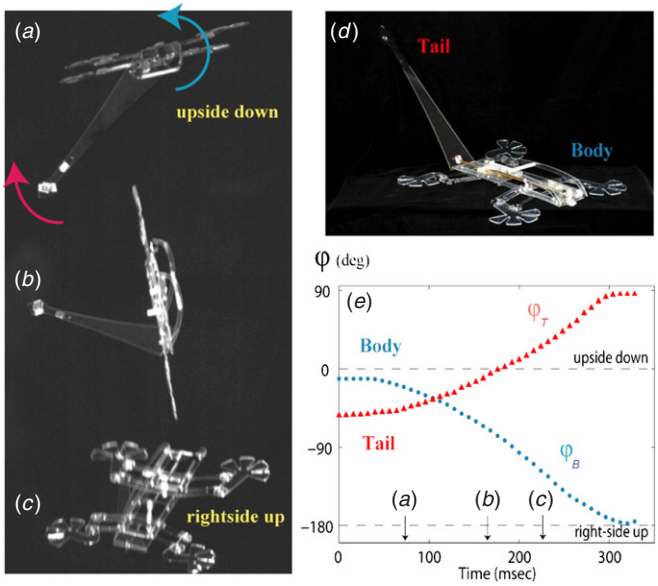

Figure 5. Air-righting maneuver performed by the robot prototype. The tail was rotated about the robot's longitudinal axis. (*a*) Free falling robot begins in upside-down pose. The tail (red arrow) rotates clockwise and the body (blue) anti-clockwise. Reorientation is initiated after a characteristic latency upon take-off. (*b*) Robot mid-way during air righting. (*c*) Robot attained right-side-up posture more favorable for collision with the ground. (*d*) Dorso-lateral view of the robot prototype showing its similarity to Stickybot [24]. (*e*) Plot depicts robot's body (•, φ_B) and tail (▲, φ_T) rotation as a function of time (see figures 1(*f*) and 3(*b*)).

Second, we explored the parameter space beyond the house gecko to predict how further increases in tail length might affect turning (figure 4). Anoles with short tails (tail length/body length = 1.57) need to sweep their tail by 90° to turn their body by about 20°. If, however, they swing their tail 180°, then the body should turn by over 40°. By contrast, if the tail is nearly twice as long as the average house gecko, similar to that found in the green anole *A. carolinensis* (tail length = 10.5 cm, tail length/body length = 2.29) and it is swung 90°, then the body should yaw over 40°. A tail swing of 180° for the same morphology should yield a turn of the body of over 80°. Again, the model predicts the increased effectiveness of a relatively longer caudal appendage.

3.3. Model scaling

We used our analytical model to speculate on the effects scaling has on aerial maneuvers and to assist in the design of our robot prototype. Suppose we scale lengths by a length ratio $\alpha = L'/L$, where L is the nominal length and L' is the scaled length. Clearly, $L' = \alpha L$. Assuming constant density across all size scales, mass is proportional to volume, and hence the scaled mass m' is related to the nominal mass m by $m' = \alpha^3 m$. Since moment of inertia has units of mass times length squared, the inertias of the body and tail scale as $J' = \alpha^5 J$. From equations (1) and (B.6)–(B.20), we observe that every term of the coefficient matrix $\mathbf{A}$ and the coefficient vectors $\mathbf{f}_1$ and $\mathbf{f}_2$ is multiplied by a moment of inertia (J_{b1}, J_{t1}, etc) or an inertia-like term (e.g. mL_1L_2). The scaling appears on both sides of the equations of motion as α^5 and thus cancels out, from which we conclude that isometric scaling has no effect on the dynamical response of the system. A given tail rotation should elicit a corresponding body rotation irrespective of size.

Assuming no storage/return of energy in elastic tissues, the total work required to complete the maneuver must equal twice the maximum rotational kinetic energy (proportional to mass moment of inertia) of the body and tail and hence scales as α^5. To maintain constant righting duration, the average mass-specific power supplied by the actuator must increase as α^2 and hence we hypothesize that time of righting will increase at larger size scales.

3.4. Robot prototype

Rather than producing a physical model of the size of the house gecko, *H. platyurus,* we chose to explore the analytical model's predictions by building a relevant robot prototype with the size and morphology of the most effective climbing robot (figure 5). Stickybot, a quadrupedal robot inspired by the morphology and dynamics of house geckos, can climb smooth vertical surfaces [26]. We anticipate that one of the next steps in its development will be mid-air reorientation, perhaps allowing directed aerial descent.

Our robot prototype completed a mid-air righting behavior similar to that observed in the geckos and predicted by our analytical model. As the tail of the robot accelerated, the body rotated in the opposite direction by 180° in 250–300 ms (figures 5(*a*)–(*c*) and (*e*)). After the maneuver ended with the tail at rest with respect to the body, no further rotation was observed (see movie 7 available at stacks.iop.org/BB/5/045001/mmedia, figure 5(*d*)) before the model collided with the ground, indicating that no net angular momentum was introduced by the release process or by drag.

Analytical model predictions agreed with observed robot behavior even though the analytical model differed in

morphology (tables 2 and 3). Using the nominal measured physical parameters, the model predicted a body roll of 148.7° and residual nose-up pitch of 34.2°. The observed roll of the robot prototype was 168° with approximately 30° of pitch. Flexing of the body and tail in the physical model during the rotation may account for some of the differences between the predicted and observed rotation.

The robot prototype was designed with an inclined tail angle (35°) to avoid potential collisions with the hind legs in the real robot. To achieve complete righting with the inclined tail, we used a relatively large tail moment of inertia. The tail moment of inertia taken about its base for the gecko (6.8×10^{-8} kg m^2) was nearly equal to the body roll moment of inertia. In our robot, the moment of inertia about the base was 2.4×10^{-3} kg m^2, nearly four-fold larger than the roll moment of inertia. The necessarily larger tail moment of inertia in the robot is consistent with the analytical model's prediction that longer tails would be necessary in animals using inclined tails. However, since the tail was not constrained to conical morphology, we were able to effect the necessary change in the moment of inertia without lengthening the tail or increasing mass significantly. If a conical tail morphology were used in the robot with the same mass and dimensions, the moment of inertia about the tail base would be 5.64×10^{-4} kg m^2, less than 25% of the value needed for complete righting. If the robot's tail is orthogonal to the body, as in the average gecko, the predicted roll by the analytical model increases to 221°.

The performance of our robot prototype underscores the effectiveness of air righting with redistribution of mass using tail rotation, thus complementing the results of our theoretical analysis. By contrast, Mather and Yim's [27] analysis of a modular robot's controlled fall led them to conclude that 'tail-type inertias are not potentially useful'. Their two-joint robot, with essentially a flexible spine, self-rights via cat-like back-bending rotations. The authors speculate that tail-like devices attached to the end of a body will be ineffective because of the large inertial load that they must move. We agree that segmenting a body and reorienting by cat-like twisting could reduce the inertial load. However, our animal and robot prototype data do not support the assertion that tails are necessarily useless because body bending has a particular advantage. Tails provide an opportunity for simple body attitude control with a single swing or sweep, whereas back twisting from an arbitrary initial orientation is a far more challenging control problem, may take longer to execute and is less likely to attain the desired body position with all the legs from each segment safely on the ground or wall. Also, as pointed out in Mather and Yim [27], 'tail-type inertia loads do have a significant advantage in that their final orientation is usually unimportant to the system'. Moreover, tails can be easily added to current platforms and have been shown to have the added benefit of vertical climbing stabilization [26]. Finally, we observe that tail-like structures can be economical with respect to mass; in geckos, the tail was on average only 1/10th of the body mass, yet still enabled the fastest air righting yet observed in an animal or robot. In fact, a solution using inertial appendages could simplify control of a variety of unmanned aerial and space vehicles, because it allows for reorientation without the need to implement complex, multi-axis bending or twisting of the trunk [32].

4. General conclusions

Addition of an appendage to a body allows rapid rotations about a chosen axis. Our model predictions indicate that a simple two-link system (i.e. body and tail) with a two degree-of-freedom joint enables effective attitude control of the body without the need for external work. Such a system can maintain rotational control authority in the absence of an environment on which it can generate forces. An airborne animal or robot could maintain control authority at zero airspeed or high angles of attack, where lift-based control mechanisms can generate little or no force.

The utility of an inertial appendage extends beyond the aerial rotations illustrated here. Undesired angular momentum injected by disturbances could be temporarily directed to the appendage, allowing the body to remain stable until substrate interactions allow dissipation of the perturbation energy. Modulating the mechanical properties of the joint could effect large changes in the dynamical behavior of the system. For example, traditional aircraft with fixed body structures must compromise between stability and maneuverability. By varying the stiffness and position of an appendage such as a tail, the aircraft could modulate the moment of inertia about arbitrary axes of rotation, allowing it to rapidly change from a stable mode to a maneuverable mode. Terrestrial or scansorial robots could use such an appendage to generate transient torques to maintain body attitude in the face of unsteady or unpredictable surface forces.

Acknowledgments

We thank Robert Dudley, Daniel Goldman, Shai Revzen, Justin Seipel and Simon Sponberg for helpful suggestions and insights. We thank Pauline Jennings, Edward Tufte and Attila Bergou for creative input on the artwork. Research was partially supported by a Swiss NSF Fellowship for Prospective Researchers to AJ as well as by a grant from NSF FIBR (EF-0425878) to RJF and ARL MAST CTA (W911NF-08-2-0004). We also thank two anonymous reviewers for their constructive comments that have improved this paper.

Appendix A. Estimating the maximum drag moment acting on the gecko during air righting

To estimate the maximum drag moment acting on the gecko while it performs its air-righting maneuver, we consider the simplified case in which the body and tail are held orthogonal to each other. The effects of pitch and yaw are very small for this alignment of tail and body, so we assume that rotation occurs solely in the vertical *XZ* plane. Also, it is assumed that the gecko executes a perfect reorientation: the body rotates 180°. The passive falling speed of the body at the beginning of free fall is small relative to the body and tail rotation by muscle power. Moreover, the tail is rotating upward and in the opposite direction to the downward falling body. Consequently, we

ignore the oncoming airflow due to free fall and consider just the airflow tangent to the rotating tail and body. In essence, we are calculating our estimate of the drag moment from a model in which the body and tail rotate about a common pivot fixed in space, where the pivot coincides with the base of the tail and the centerline of the body. For brevity, we detail here the analytical methods for estimating the maximum drag moment acting on the tail only—the drag moment acting on the body (torso and legs) is determined in a similar fashion. We then compare the tail drag moment to the moment associated with air righting.

Because of the geometry of the projected (frontal) area of the tail and the variation in speed of the oncoming airflow, the applied drag force will vary along the rotating tail. Since the tail is modeled as a cone, its projected area is an isosceles triangle with base width $2R$ (where R is the tail base radius) and height L_t (tail length), and hence the projected area varies linearly in width from base to tip. The tail spins about its base with angular speed ω, and so the speed of the oncoming tangential airflow increases linearly from the base, where the air speed is zero, to the tail tip, where the air speed is a maximum at ωL_t. Let h denote the distance along the tail's length from its base. The differential aerodynamic drag force $\mathrm{d}F_D$ acting on the tail is

$$\mathrm{d}F_D = \tfrac{1}{2}\rho C_D v(h)^2\,\mathrm{d}A, \tag{A.1}$$

where the air density $\rho = 1.2$ kg m^{-3}, C_D is the drag coefficient (assumed constant), $v(h)$ is the variation in oncoming airflow and $\mathrm{d}A$ is the differential projected area:

$$v(h) = \omega h, \tag{A.2}$$

$$\mathrm{d}A = 2R\left(1 - \frac{h}{L_t}\right)\mathrm{d}h. \tag{A.3}$$

The corresponding net drag moment M_D acting at the tail pivot is determined by integration over the tail length:

$$M_D = \int h\,\mathrm{d}F_D. \tag{A.4}$$

For simulation, we used a half-cosine profile for the absolute rotation of the tail based on the experimental data for tail sweep trajectory in figure 1(f):

$$\varphi_T(t) = -\frac{\pi}{2}\cos\left(\frac{\pi}{t_f}t\right), \tag{A.5}$$

where $t_f = 110$ ms is the average duration of air righting based on experimental observations. Differentiation of equation (A.5) gives a maximum angular speed and acceleration of $\omega_{\max} = \pi^2/(2t_f)$ and $\dot{\omega}_{\max} = \pi^3/(2t_f^2)$, respectively. Integrating equation (A.4) and evaluating at the maximum angular speed, the maximum drag moment acting at the tail pivot is

$$M_{D,\max} = \frac{\rho C_D R\,(\pi L_t)^4}{80 t_f^2}. \tag{A.6}$$

Using a drag coefficient $C_D = 1$ for a smooth cylinder and the average parameter values given in table 2, we obtain $M_{D,\max} = 3.02 \times 10^{-6}$ N m. This value is an overestimate for several reasons. First, we used a drag coefficient for a cylinder, not a cone. Because of the taper of the cone, the drag coefficient is not uniform across the tail and decreases toward the tip (since the tail becomes more like a thin plate). Second, looking at the compressed tail of the flat-tailed house gecko from the side, its base width is a fraction of $2R$. Since the flatter side of the tail is presented to the oncoming airflow during air righting, using the maximal width $2R$ for calculation gives an overestimate of $M_{D,\max}$. The maximum drag moment acting on the torso and legs can be approximated in the same manner as for the tail, yielding a value of $M_{b,\max} = 1.79 \times 10^{-7}$ N m, an order of magnitude lower than the maximum drag moment exerted on the tail.

Next we compare the maximum value of the drag moment to the maximum moment needed to spin the body around by 180°. This air-righting moment $M_{I,\max}$ is obtained by a moment balance on the body around the mutual pivot for the body and tail:

$$M_I = J_{\text{body,pivot}}\dot{\omega} = J_{b2}\dot{\omega}, \tag{A.7}$$

where J_{b2} is the moment of inertia of the body about its mass center. The drag moment M_b acting on the body would normally be added to the right-hand side of equation (A.7), but it has been neglected because its maximum value $M_{b,\max}$ is two orders of magnitude smaller than the maximum inertial term $J_{b2}\dot{\omega}_{\max}$, implying that body drag is an insignificant effect. Using the average value of J_{b2} listed in table 2, an estimate of the maximum moment exerted for air righting is $M_{I,\max} = 8.47 \times 10^{-5}$ N m. Comparing the drag and inertial moments, we find that $M_{D,\max} = 0.036 M_{I,\max}$, or the maximum moment induced by tail drag is estimated to be 3.6% of the maximum moment that the geckos require to perform air righting.

Appendix B. Derivation of the equation of motion

Let $\{\mathbf{E}_1, \mathbf{E}_2, \mathbf{E}_3\}$ be a set of basis vectors for the ground-fixed frame XYZ. Likewise, take $\{\mathbf{b}_1, \mathbf{b}_2, \mathbf{b}_3\}$ to be a set of basis vectors for the frame $x_b y_b z_b$ attached to and rotating with the gecko body. Using a set (ψ, θ, φ) of 3–1–2 Euler angles to parameterize the rotation of the gecko body, the ground-fixed vectors are rotated into the body-fixed vectors according to

$$\begin{bmatrix}\mathbf{b}_1\\ \mathbf{b}_2\\ \mathbf{b}_3\end{bmatrix} = \begin{bmatrix}C_\varphi & 0 & -S_\varphi\\ 0 & 1 & 0\\ S_\varphi & 0 & C_\varphi\end{bmatrix}\begin{bmatrix}1 & 0 & 0\\ 0 & C_\theta & S_\theta\\ 0 & -S_\theta & C_\theta\end{bmatrix} \times \begin{bmatrix}C_\psi & S_\psi & 0\\ -S_\psi & C_\psi & 0\\ 0 & 0 & 1\end{bmatrix}\begin{bmatrix}\mathbf{E}_1\\ \mathbf{E}_2\\ \mathbf{E}_3\end{bmatrix}, \tag{B.1}$$

where $S_\alpha = \sin\alpha$ and $C_\alpha = \cos\alpha$ for any angle α. The body's total angular velocity vector $\boldsymbol{\omega}_b$ has components $\omega_{bi} = \boldsymbol{\omega}_b \cdot \mathbf{b}_i$ $(i = 1, 2, 3)$ in the body-fixed basis given by

$$\begin{aligned}\omega_{b1} &= -\dot{\psi}S_\varphi C_\theta + \dot{\theta}C_\varphi,\\ \omega_{b2} &= \dot{\psi}S_\theta + \dot{\varphi},\\ \omega_{b3} &= \dot{\psi}C_\varphi C_\theta + \dot{\theta}S_\varphi.\end{aligned} \tag{B.2}$$

Let $\{\mathbf{t}_1, \mathbf{t}_2, \mathbf{t}_3\}$ be a set of basis vectors for the frame $x_t y_t z_t$ fixed on the tail. Based on the sequence of rotations depicted in figures 2(e) and (f) for the side sweep η and the inclination

γ of the tail relative to the body, the tail-fixed vectors are related to the body-fixed vectors by the transformation

$$\begin{bmatrix}\mathbf{t}_1\\ \mathbf{t}_2\\ \mathbf{t}_3\end{bmatrix}=\begin{bmatrix}1 & 0 & 0\\ 0 & C_\gamma & S_\gamma\\ 0 & -S_\gamma & C_\gamma\end{bmatrix}\begin{bmatrix}C_\eta & 0 & -S_\eta\\ 0 & 1 & 0\\ S_\eta & 0 & C_\eta\end{bmatrix}\begin{bmatrix}\mathbf{b}_1\\ \mathbf{b}_2\\ \mathbf{b}_3\end{bmatrix}, \tag{B.3}$$

and so the total angular velocity vector of the tail is

$$\boldsymbol{\omega}_t=\boldsymbol{\omega}_b+\dot\gamma C_\eta\mathbf{b}_1+\dot\eta\mathbf{b}_2-\dot\gamma S_\eta\mathbf{b}_3. \tag{B.4}$$

From equation (2) in [30], the total angular momentum of the torso–tail system about its mass center takes the form

$$\mathbf{H}=\mathbf{J}_b\boldsymbol{\omega}_b+\mathbf{J}_t\boldsymbol{\omega}_t+\frac{m_bm_t}{m_b+m_t}(\boldsymbol{\xi}\times\dot{\boldsymbol{\xi}}), \tag{B.5}$$

where the inertia tensors $\mathbf{J}_b$ and $\mathbf{J}_t$ are symmetric, and m_b and m_t are the total body mass (torso and legs) and tail mass, respectively. The vector $\boldsymbol{\xi}=L_1\mathbf{b}_2+L_2\mathbf{t}_3$ is the relative position vector between the centers of mass of the body and tail. The distance along the body's length between its mass center and the center of the tail's base is L_1, and L_2 is the distance between the center of the tail's base and its center of mass. By setting equation (B.5) to zero to conserve angular momentum and taking components in the body-fixed frame $x_by_bz_b$, we obtain the equation of motion (1) with components A_{ik} $(i,k=1,2,3)$ of the coefficient matrix $\mathbf{A}$ given by

$$\begin{aligned}A_{11}=&\tfrac{1}{4}\big[2S_\eta\big(J_{t2}-J_{t3}+mL_2^2\big)(S_{2\gamma}S_\theta-C_{2\gamma}C_{\varphi\eta}C_\theta)\\&+4mL_1L_1(2C_\theta S_\gamma S_\varphi-C_\gamma S_\eta S_\theta)\\&-C_\theta\big(4C_\eta S_{\varphi\eta}J_{t1}+4S_\varphi\big(J_{b1}+mL_1^2\big)\\&-2C_{\varphi\eta}S_\eta(J_{t2}+J_{t3})+mL_2^2(S_{2\eta\varphi}+3S_\varphi)\big)\big],\end{aligned} \tag{B.6}$$

$$\begin{aligned}A_{12}=&C_\varphi J_{b1}+C_\eta C_{\varphi\eta}J_{t1}+m[C_\eta C_{\varphi\eta}(C_\gamma L_2)^2\\&+C_\varphi(L_1-L_2S_\gamma)^2]+S_\eta S_{\varphi\eta}\big(J_{t3}C_\gamma^2+J_{t2}S_\gamma^2\big),\end{aligned} \tag{B.7}$$

$$A_{13}=C_\gamma S_\eta\big[\big(J_{t2}-J_{t3}+mL_2^2\big)S_\gamma-mL_1L_2\big], \tag{B.8}$$

$$\begin{aligned}A_{21}=&J_{t2}C_\gamma(C_\gamma S_\theta+C_{\varphi\eta}C_\theta S_\gamma)+J_{t3}S_\gamma(S_\gamma S_\theta-C_{\varphi\eta}C_\theta C_\gamma)\\&+mL_2C_\gamma[L_2(C_\gamma S_\theta+C_{\varphi\eta}C_\theta S_\gamma)\\&-C_{\varphi\eta}C_\theta L_1]+J_{b2}S_\theta,\end{aligned} \tag{B.9}$$

$$A_{22}=C_\gamma S_{\varphi\eta}\big[\big(J_{t2}-J_{t3}+mL_2^2\big)S_\gamma-mL_1L_2\big], \tag{B.10}$$

$$A_{23}=J_{b2}+\big(J_{t2}+mL_2^2\big)C_\gamma^2+J_{t3}S_\gamma^2, \tag{B.11}$$

$$\begin{aligned}A_{31}=&\tfrac{1}{4}\big[2C_\eta\big(J_{t2}-J_{t3}+mL_2^2\big)(S_{2\gamma}S_\theta-C_{2\gamma}C_{\varphi\eta}C_\theta)\\&-4mL_1L_1(C_\gamma C_\eta S_\theta+2C_\theta S_\gamma C_\varphi)\\&+C_\theta\big(4S_\eta S_{\varphi\eta}J_{t1}+4C_\varphi\big(J_{b3}+mL_1^2\big)+2C_{\varphi\eta}C_\eta(J_{t2}+J_{t3})\\&-mL_2^2(C_{2\eta\varphi}-3C_\varphi)\big)\big],\end{aligned} \tag{B.12}$$

$$\begin{aligned}A_{32}=&S_\varphi J_{b3}-S_\eta C_{\varphi\eta}J_{t1}+m[S_\varphi(L_1-L_2S_\gamma)^2\\&-S_\eta C_{\varphi\eta}(C_\gamma L_2)^2]+C_\eta S_{\varphi\eta}\big(J_{t3}C_\gamma^2+J_{t2}S_\gamma^2\big),\end{aligned} \tag{B.13}$$

$$A_{33}=C_\gamma C_\eta\big[\big(J_{t2}-J_{t3}+mL_2^2\big)S_\gamma-mL_1L_2\big]. \tag{B.14}$$

The components f_{1i} $(i=1,2,3)$ of the vector $\mathbf{f}_1$ associated with the tail side sweep are

$$f_{11}=-C_\gamma S_\eta\big[\big(J_{t2}-J_{t3}+mL_2^2\big)S_\gamma-mL_1L_2\big], \tag{B.15}$$

$$f_{12}=-\big(J_{t2}+mL_2^2\big)C_\gamma^2-J_{t3}S_\gamma^2, \tag{B.16}$$

$$f_{13}=-C_\gamma C_\eta\big[\big(J_{t2}-J_{t3}+mL_2^2\big)S_\gamma-mL_1L_2\big]. \tag{B.17}$$

The components f_{2i} $(i=1,2,3)$ of the vector $\mathbf{f}_2$ associated with tail inclination are

$$f_{21}=-C_\eta[J_{t1}+mL_2(L_2-L_1S_\gamma)], \tag{B.18}$$

$$f_{22}=0, \tag{B.19}$$

$$f_{23}=S_\eta[J_{t1}+mL_2(L_2-L_1S_\gamma)]. \tag{B.20}$$

In these equations, $S_{2\alpha}=\sin2\alpha$, $C_{2\alpha}=\cos2\alpha$, $S_{\alpha\beta}=\sin(\alpha+\beta)$, $C_{\alpha\beta}=\cos(\alpha+\beta)$, $S_{2\alpha\beta}=\sin(2\alpha+\beta)$ and $C_{2\alpha\beta}=\cos(2\alpha+\beta)$ for any two angles α and β. Also, J_{bi} $(i=1,2,3)$ and J_{ti} denote the moments of inertia for the body and tail, respectively, about their mass centers, where $J_{t1}=J_{t2}$ for the conical tail. In addition, $m=m_bm_t/(m_b+m_t)$ for convenience.

References

[1] Jurmain R 1997 Skeletal evidence of trauma in African apes, with special reference to the gombe chimpanzees *Primates* **38** 1–14

[2] Nakai M 2003 Bone and joint disorders in wild Japanese macaques from Nagano Prefecture, Japan *Int. J. Primatol.* **24** 179–95

[3] Sinervo B and Losos J B 1991 Walking the tight rope: arboreal sprint performance among *Sceloporus occidentalis* lizard populations *Ecology* **72** 1225–33

[4] Knops J M H, Schlesinger W H and Nash T H 1993 Arboreal sprint failure: falling lizards in California blue oak woodlands *Bull. Ecol. Soc. Am.* **74** (2 suppl.) 313

[5] Marey E J 1894 Des mouvements que certains animaux exécutent pour retomber sur leurs pieds, lorsqu'ils sont précipités d'un lieu élevé *C. R. Acad. Sci., Paris* **119** 714–7

[6] Magnus R 1922 Wie sich die fallende katze in der luft umdreht *Arch. Néerl. Physiol.* **7** 218–22

[7] McDonald D A 1960 How does a cat fall on its feet? *New Sci.* **7** 1647–9

[8] Kane T P and Scher M P 1969 A dynamical explanation of the falling cat phenomenon *Int. J. Solids Struct.* **5** 663–70

[9] Edwards M H 1989 Zero-angular momentum turns *Am. J. Phys.* **54** 846–7

[10] Arabyan A and Tsai D 1998 A distributed control model for the air-righting reflex of a cat *Biol. Cybern.* **79** 393–401

[11] Marsden J E and Ostrowski J 1998 Symmetries in motion: geometric foundations of motion control *Nonlinear Sci. Today*

[12] Schönfelder J 1984 The development of air-righting reflex in postnatal growing rabbits *Behav. Brain Res.* **11** 213–21

[13] Laouris Y, Kalli-Laouri J and Schwartze P 1990 The postnatal development of the air-righting reaction in albino rats. Quantitative analysis of normal development and the effect of preventing neck–torso and torso–pelvis rotations *Behav. Brain Res.* **37** 37–44

[14] Pellis S M, Pellis V C, Morrissey T K and Teitelbaum P 1989 Visual modulation of the vestibularly-triggered air-righting in the rat *Behav. Brain Res.* **35** 23–6

[15] Kane T P and Scher M P 1970 Human self-rotation by means of limb movements *J. Biomech.* **3** 39–49

[16] Dunbar D C 1988 Aerial maneuvers of leaping lemurs: the physics of whole-body rotations while airborne *Am. J. Phys. Anthrop.* **16** 291–303
[17] Demes B *et al* 1996 Body size and leaping kinematics in Malagasy vertical clingers and leapers *J. Hum. Evol.* **31** 367–88
[18] Larson and Stern 2006 Maintenance of above-branch balance during primate arboreal quadrupedalism: coordinated use of forearm rotators and tail motion *Am. J. Phys. Anthrop.* **129** 71–81
[19] Essner R L 2002 Three-dimensional launch kinematics in leaping, parachuting and gliding squirrels *J. Exp. Biol.* **205** 2469–77 16
[20] Wassersug R J *et al* 2005 The behavioural responses of amphibians and reptiles to microgravity on parabolic flights *Zoology (Jena)* **108** 107–20
[21] Oliver J A 1951 'Gliding' in amphibians and reptiles, with a remark on an arboreal adaptation in the lizard, *Anolis carolinensis carolinensis Am Nat.* **85** 171–6
[22] Young B A, Lee C E and Daley K A 2002 On a flap and a foot: aerial locomotion in the 'flying' gecko, *Ptychozoon kuhli J. Herpetol.* **36** 412–8
[23] Higham T E, Davenport M S and Jayne B C 2001 Maneuvering in an arboreal habitat: the effects of turning angle on the locomotion of three sympatric ecomorphs of Anolis lizards *J. Exp. Biol.* **204** 4141–55
[24] Gillis G B, Bonvini L A and Irshick D J 2009 Loss of stability: tail loss and jumping in the arboreal lizard Anolis carolinensis *J. Exp. Biol.* **212** 604–9
[25] Jusufi A, Goldman D I, Revzen S and Full R J 2008 Active tails enhance arboreal acrobatics in geckos *Proc. Natl Acad. Sci. USA* **105** 4215–19
[26] Kim S, Spenko M, Trujillo S, Heyneman B, Mattoli V and Cutkosky M R 2007 Whole body adhesion: hierarchical, directional and distributed control of adhesive forces for a climbing robot *IEEE ICRA07*
[27] Mather T W and Yim M 2009 Modular configuration design for a controlled fall 2009 *IEEE/RSJ Int. Conf. on Intelligent Robots and Systems* pp 5905–10
[28] Fernandes C, Gurvits L and Li Z 1994 Near-optimal nonholonomic motion planning for a system of coupled rigid bodies *IEEE Trans. Autom. Control* **39** 450–63
[29] Li Z and Montgomery R 1990 Dynamics and optimal control of a legged robot in flight phase *IEEE Int. Conf. on Robotics and Automation* pp 1816–21
[30] Passerello C E and Huston R L 1971 Human attitude control *J. Biomech.* **4** 95–102
[31] Yang E C-Y, Chao P C-P and Sung C-K Optimal control of an under-actuated system for landing with desired postures *IEEE Trans. Control Syst. Technol.* at press
[32] Kane T P and Scher M P 1969 A method of active attitude control based on energy considerations *J. Spacecr. Rockets* **6** 633–6